A Quantitative Determination of the Conditions for Hot Cracking During Welding for Aluminum Alloys

A combination of strain and susceptible microstructure causes failure which occurs preferentially in the heat-affected zone adjacent to the weld bead

BY J. E. STEENBERGEN AND H. R. THORNTON

ABSTRACT. A quantitative correlation is made to determine the conditions for hot cracking in aluminum alloys. A combination of strain and susceptible microstructure is determined as the cause of the failure, which occurs preferentially in the heat-affected zone adjacent to the weld bead. Aluminum alloys, 6061-T6 and 7075-T6, were simulated weld tested, analyzed for developed strains, and compared with the microstructure of the specimen. An elastic-plastic strain interaction is outlined as the cause of hot cracking in aluminum alloys.

Introduction

The demands of industry, particularly the aerospace industry, for structural materials with high strength-to-weight ratios are constantly increasing. However, the use of these materials had been greatly restricted by the failures of welded components made from these materials. Although there is an extensive backlog of welding experience which is applicable to the problem of these failures, it is difficult to predict the weld behavior of a material during the production of a completed part.

When the complexity of the metallurgical and mechanical factors which affect a weld are considered, it is easy to understand why an accurate prediction of weld behavior cannot be made. If the large number of variables involved in a welding process can be reduced to a few fundamental parameters, a quantitative relationship between these parameters and their effect on a weld can be ascertained.

J. D. STEENBERGEN is with Union Carbide Corp., Chemicals and Plastics Div., Texas City, Tex., and was a Research Assistant, Dept., of Mechanical Engineering, Texas A & M University, College Station, Tex.; H. R. THORNTON is Associate Professor, Dept. of Mechanical Engineering, Texas A & M University.

Based in part on a thesis submitted for the M. S. degree in Interdisciplinary Engineering at Texas A & M University and supported by a grant from the Welding Research Council of the Engineering Foundation.

An important group of high strength-to-weight materials is the aluminum alloys. These alloys present attractive mechanical properties to the designer but also encounter a welding phenomenon known as hot cracking. The presence of this failure phenomenon limits the applicability of aluminum alloys. Knowledge of the mechanism of hot cracking would provide a quantitative structure which would enhance the applicability of these alloys.

General Considerations

Two types of hot cracks can be defined on the basis of their characteristic location. These are:

1. The interface weld between two components.
2. The heat-affected zone adjacent to the interface weld.

Published research[1-5] has yielded a common factor; hot cracking is invariably associated with the heat-affected zone. The weld heat-affected zone is defined as: "that portion of the base metal which has not been melted, but whose mechanical properties or microstructure have been altered by the heat of welding or cutting."[6] The unmelted base metal in this region experiences thermal cycles that result from the rapid heating and cooling produced by the welding process. These cycles range in temperature from just above the equilibrium solidus temperature to ambient temperature. The hot cracks in the heat-affected zone are related to microsegregation within the grain boundaries. These solute rich regions are preferential sites for crack initiation and propagation.[7]

Several theories[8-10] have been proposed to explain the hot cracking behavior within the heat-affected zone. Borland[11] combined and extended these theories into a generalized theory which attempts to explain how the liquid quantity and distribution during freezing affects the cracking tendency. Thi generalized theory postulates that it i not sufficient that a wide freezing range exist for cracking to occur, but that the liquid phase be present in a form that will allow high stresses to be generated between grains. The distribution and quantity of the liquid phase present is influenced by the grain size and shape and the effect of temperature and cooling rate on the liquidus and solidus temperatures. The net effect establishes the hot cracking tendency.

More recent studies by Bell[12] and Savage[7] verify Borland's theory in general but also indicate that hot cracking is caused by a combination of mechanical strain and susceptible microstructure. The mechanical strain is the result of restraint against thermal contraction by external fixturing and is affected by solute segregation.

The large amount of information that has been generated on hot cracking can be reduced to the following basic facts:

1. The mechanical effects relating to crack susceptibility are reduced to the primary factor of restraint.
2. The cooling rate and the peak (maximum) temperature are the principal thermal considerations.
3. The grain size, shape and segregation are the basic metallurgical variables.

The interaction of the mechanical, thermal and metallurgical effects on hot crack susceptibility has not been rigidly defined. The understanding of this interaction establishes the utility of welded structural metal.

Theoretical Approach

The formulation of a theory to describe the interaction of the mechanical, thermal and metallurgical effects on hot crack susceptibility is outlined for aluminum alloys. Wells,[13] in the strain

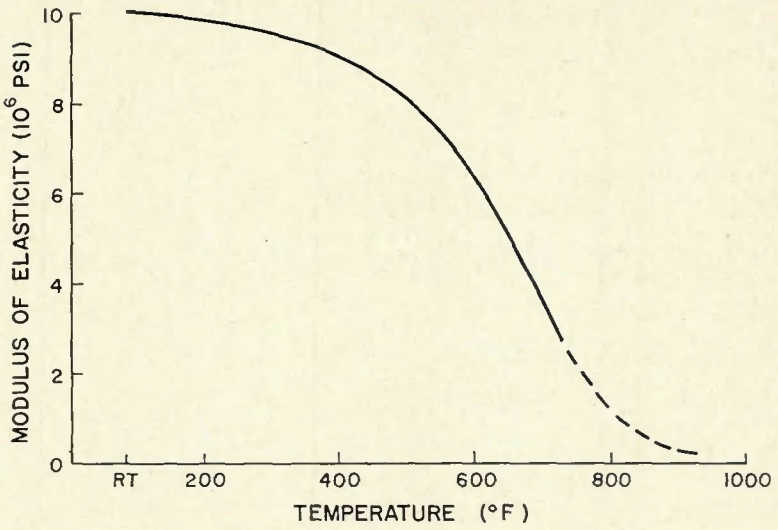

Fig. 1—Typical modulus of elasticity vs. temperature relationship for aluminum alloys

duplication method, considers the generation of strain in the temperature region between the heating solidus (T_s) and the cooling solidus (T_c) using the uniaxial strain equation:

$$\lambda = \alpha \Delta T + S_x/E + \epsilon_x \qquad (1)$$

where: λ = total strain (in./in.); α = coefficient of thermal expansion (in./in./°F); $\Delta T = T_s - T_c$ (°F); S_x/E = elastic strain from load (in./in.); ϵ_x = plastic strain (in./in.).

The equation approximates accountable strain at the cooling solidus temperature.

The basic parameters contributing to hot cracking within the heat-affected zone during welding have been clearly defined. These parameters include restraint, cooling rate, and peak temperature of the thermal cycle. The interaction of these parameters has been the subject of much research. However, existing studies, which involve both experimental and theoretical methods, have not adequately established the hot cracking mechanism.

A simulated weld (heat-affected zone) model is presented to outline the total strain at the cooling solidus. The uniaxial model is heated to a peak temperature (near the equilibrium solidus) expanding freely. At this point, the model is restricted and allowed to contract as the temperature is lowered at a specified rate. The restraint followed by contraction generates an accountable load related to cooling time and temperature. This simulation reproduces the conditions present in many weld techniques.

A plastic strain theory is presented to outline the interaction during cooling contraction. The general form:

$$\lambda = \epsilon_E + \epsilon_p + \epsilon_1 + \epsilon_2 \qquad (2)$$

where: λ = total strain (in./in.); ϵ_E = elastic strain above T_c (in./in.); ϵ_p = plastic strain above T_c (in./in.); ϵ_1 = elastic strain below T_c (in./in.); ϵ_2 = plastic strain below T_c (in./in.).

The equation takes the form of a creep strain equation. The influence of the plastic strain in the region above T_c determines crack susceptibility. This function is stress-time related and is influenced by the cooling rate. The elastic strain in this region is the sum of the uniaxial volume change associated with the phase transformation and thermal strain. The interaction between ϵ_E and ϵ_p produces the accountable strain (ϵ_c) at T_c. The interaction may be written:

$$\epsilon_c = \epsilon_E + \epsilon_p \qquad (3)$$

where: ϵ_c = total strain at T_c (in./in.); $\epsilon_E = \frac{1}{3}\frac{\Delta V}{V}\gamma + \alpha(T_p - T_c)$; γ = percent liquid phase at T_p.

Since ϵ_p is a stress-time function, ϵ_c must also be a stress-time function and is therefore effected by the peak temperature and cooling rate. The model requires that the accountable strain (ϵ_c) at T_c be determined. This can only be accomplished through knowledge of the generated load at T_c. The strain is determined as follows:

$$\epsilon_c \simeq \frac{P/A}{E} \simeq \frac{S_x}{E} \qquad (4)$$

where: P = generated load at T_c (lb); A = cross-sectional area (in.^{2}); E = modulus of elasticity at T_c (psi).

The moduli of elasticity for various temperatures can be seen in Fig. 1. The elastic modulus was assumed to be 1×10^6 psi at T_c above 800° F. Equation 4 indicates calculation of elastic strain and is used to approximate ϵ_c due to the short time intervals involved.

The thermal strain ($\alpha\Delta T$) generated below the solidus consists of both

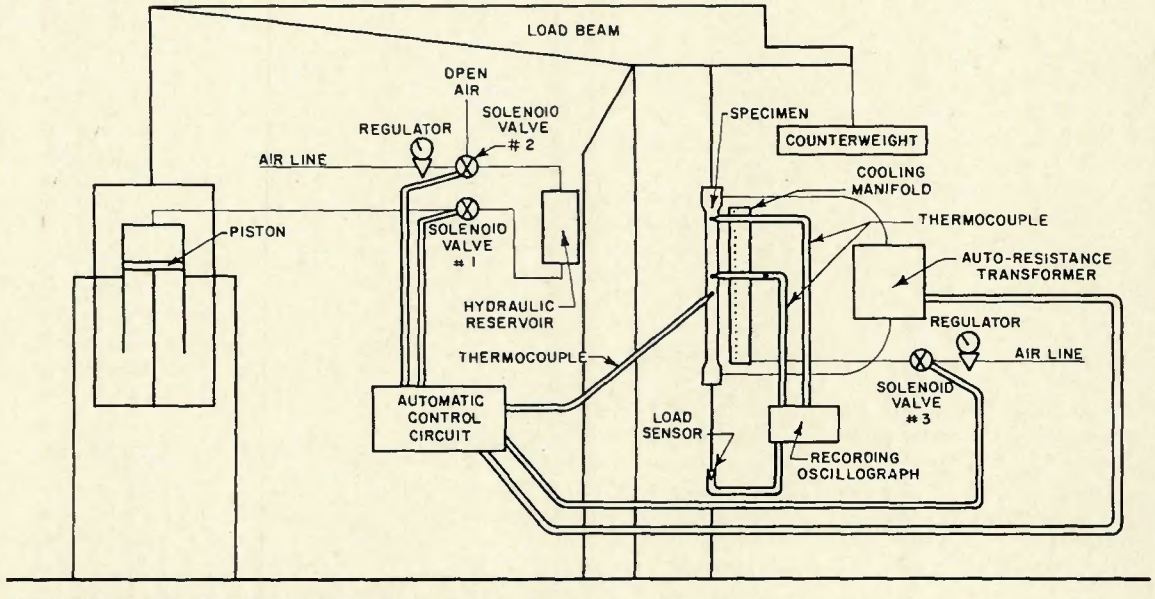

Fig. 2—Schematic diagram of strain duplication test system

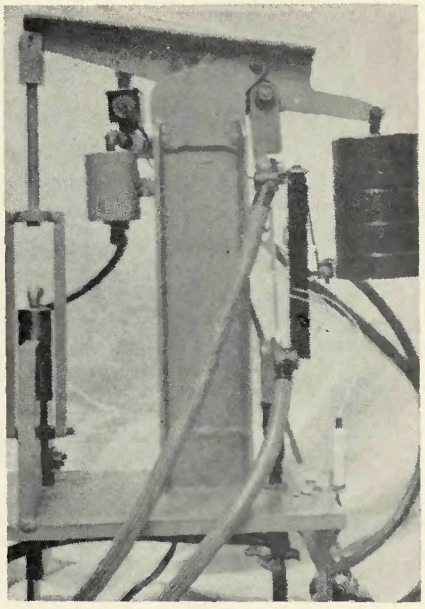

Fig. 3—The strain duplication test system

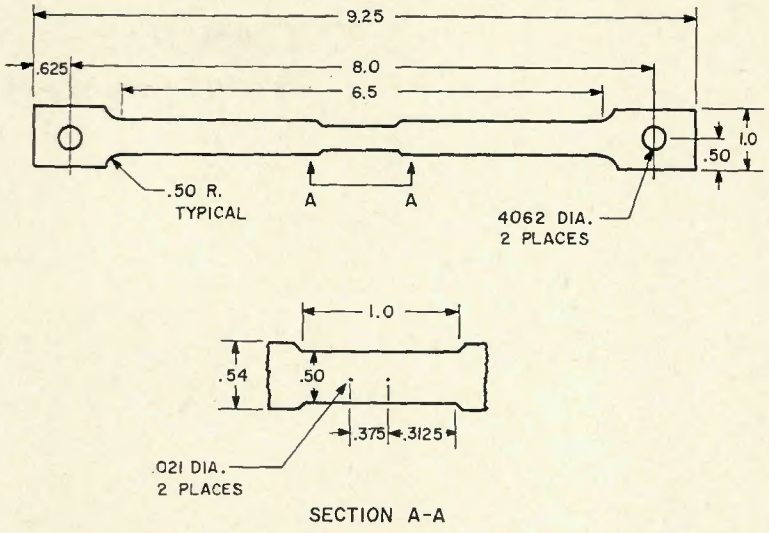

Fig. 4—Test specimen configuration. Test specimen is $^1/_8$ in. thick; dimensions are in inches

elastic (ϵ_1) and plastic (ϵ_2) strains and is a stress related function. Cooling rate does not affect the strain condition below T_c. As a result, the strains generated below T_c influence crack propagation only. The plastic strain (ϵ_2) exists when the stress level generated by the thermal stress exceeds the elastic limit, which is low at elevated temperatures. The ϵ_1 and ϵ_2 relationship is temperature dependent and vary depending on the magnitude of the $\epsilon_c + \alpha\Delta T$ strain.

Theory has indicated that the strain at or near the cooling solidus is responsible for the initiation of hot cracks during welding of aluminum alloys. This theory has been substantiated by the fact that hot cracking has been considered stress-time related. The plastic strain theory indicates an interaction of plastic and elastic strains both above and below T_c. Correlation of this theory with experimental results will define the precise expression for predicting hot cracking in aluminum alloys.

Experimentation

Several test methods[7,13] are available for use in the duplication of the heat-affected zone during welding. The intent was to incorporate an existing test method, or to develop a new test if necessary, in which the basic parameters could be varied and analyzed. The strain duplication test system was modified and refined to experimentally simulate the weld thermal cycle.

The test apparatus allows free expansion of the heated specimen until a desired peak temperature is reached, restraint of the test specimen from thermal contraction at any given point, and cooling of the specimen at selected cooling rates. The test system is shown schematically in Fig. 2 and visually in Fig. 3.

Table 1—Properties of Aluminum Alloys

Alloy	Composition, wt-%	Equilibrium liquidus, °F	Equilibrium solidus, °F	Modulus of elasticity, 10^6 psi
6061	Mg—1.0 Si—0.6 Cu—0.25 Cr—0.25	1200	1080	10.0
7075	Mg—2.5 Cu—1.5 Cr—0.3 Zn—5.5	1180	890	10.4

The metals incorporated in the study are the 6061–T6 and 7075–T6 aluminum alloys. These alloys were selected because of their usage in structural design applications and availability. The test specimen is resistance heated with a 220 V.A.C. transformer which is connected to the ends. A variable transformer is connected in series with the autotransformer to allow variation of the current. Even though the capability of varying the specimen heat-up time exists within the system, the heating rate was set at a maximum for all tests.

The free expansion of the test specimen is allowed by the balance between the counterweight and the hydraulic system. Hydraulic pressure, which is adjustable by varying the air pressure on the line, is exerted on the piston which assists in the expansion of the specimen while the counterweight keeps the specimen under a low load or slight compression condition. The proper balancing of this system insures that the

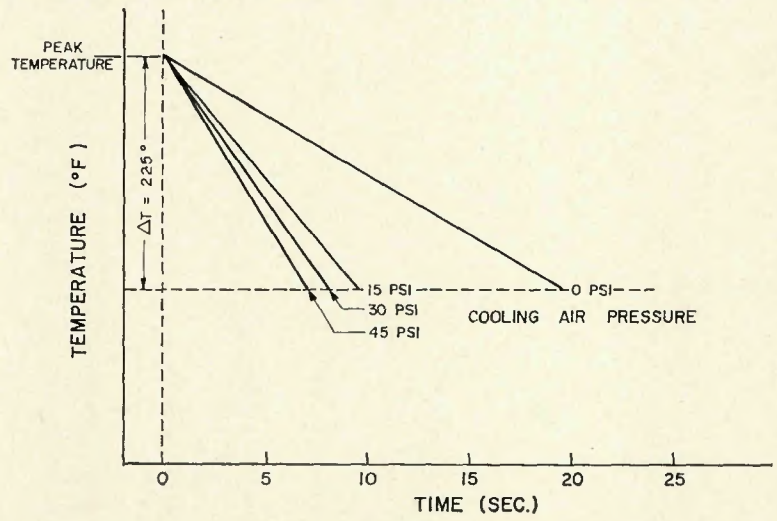

Fig. 5—Typical cooling cycles for 7075–T6 aluminum

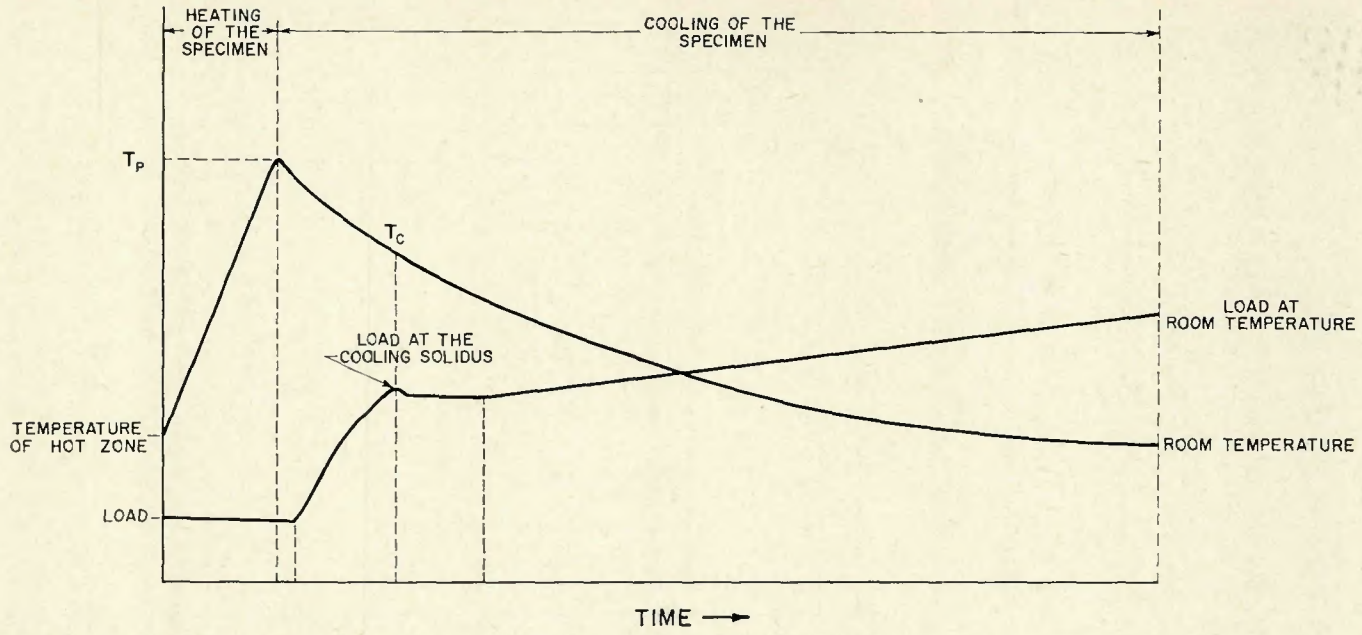

Fig. 6—Typical load-temperature data

test specimen will not fail during that portion of the heating cycle in the critical range above the solidus temperature.

The test specimen is resistance heated to a peak temperature, above the solidus temperature. The power is then turned off and the specimen allowed to cool. Various cooling rates can be easily introduced into the test by application of cooling air on to the specimen through a manifold. The cooling air pressure is controlled by a variable pressure regulator. Prior to cooling, the specimen is locked into position by closing solenoid valve #1 (Fig. 2) and restricts free contraction. The specimen is thus put into tension as it cools.

Table 2—Test Results for 6061-T6 Aluminum

Specimen number	T_p, °F	Cooling air, psi	T_c, °F	T_c load lb	R. T. load, lb	Specimen condition
1	1095	0	1015	90.84	810.18	Good
2	1095	15	979	103.11	805.27	Good
3	1095	30	830	147.00	807.00	Good
4	1105	45	915	115.39	810.18	Good
5	1135	0	1044	73.65	822.46	Good
6	1125	15	1038	81.02	817.55	Good
7	1132	30	990	103.11	748.81	Good
8	1136	45				Failure
9	1150	0				Failure

Table 3—Test Results for 7075-T6 Aluminum

Specimen number	T_p, °F	Cooling air, psi	T_c, °F	T_c load, lb	R. T. load, lb	Specimen condition
1	900	0	800	220.96	860.42	Good
2	900	15	702	306/89	1188.27	Good
3	900	30	660	370.72	845.37	Microcrack
4	900	45	640	441.92	766.00	Microcrack
5	932	0	845	208.68	1085.15	Good
6	966	15	650	478.74	932.94	Microcrack
7	939	30	639	471.38	839.64	Microcrack
8	950	45	607	326.53	684.98	Microcrack
9	990	0	840	196.41	1097.42	Microcrack
10	979	15	690	405.09	1040.96	Microcrack
11	1010	30	665	459.11	991.86	Microcrack
12	1000	45	605	503.30	1026.23	Microcrack
13	1050	0	803	245.51	1087.61	Microcrack
14	1033	15	628	491.02	1031.14	Microcrack
15	1050	30	594	540.12	1036.05	Microcrack
16	1049	45	608	564.67	1001.68	Microcrack
17	1065	0	—	—	—	Failure
18	110	15	—	—	—	Failure

The tensile load on the specimen is generated by the thermal contraction occurring under restraint. This load is detected by the use of strain gages mounted on the shaft of the lower clamp which holds the test specimen.

The test specimen was established from consideration of the basic parameters and is shown in Fig. 4. The necked down portion creates a uniform hot-zone which serves as the test area. Two thermocouples are imbedded in the test area by peening chromel-alumel thermocouples into the holes within the hot-zone. One thermocouple is connected to an automatic temperature control circuit and the other records the temperature of the test area. The temperature is recorded as a function of time in the automatic control system.

The automatic temperature controller is the heart of the control system. By setting two control points on the meter, the lower point at the temperature at which the specimen is to be restrained and the upper set point at the desired peak temperature of the hot zone, the automatic circuit turns the power on and then off, turns on the cooling air, and locks the specimen in position. The automatic control circuit allows easy variation of the test parameters as well as accurate test cycle reproduction.

The specimens were subjected to metallography following the simulated weld cycle. Photomicrographs of the various microstructures were taken and examined for grain shape and size, grain boundary phase distribution and indication of cracking.

Presentation of Data

Simulated Weld Data

The data generated with the simulated weld cycle test apparatus are pre-

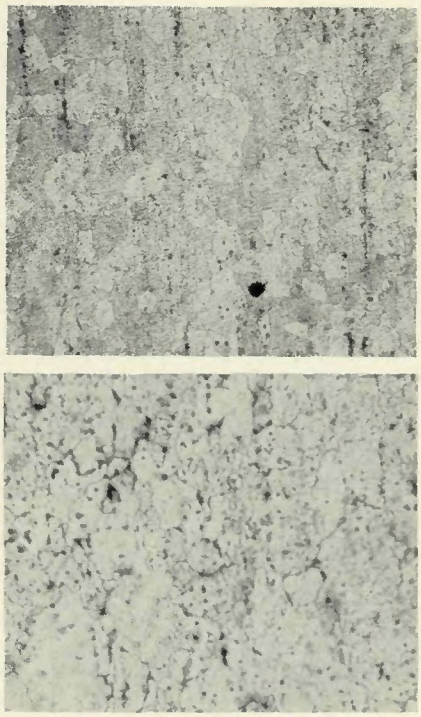

Fig. 7—As-received specimens: A (top)—6061–T6; B (bottom)—7075–T6

sented. These data include load and temperature as related to time measurements for a restrained aluminum specimen that has been cooled from a peak temperature (T_p), which is above the equilibrium solidus temperature. The peak temperature to which the heat-affected zone of the specimens was tested was determined from the properties of the specific alloy. These properties

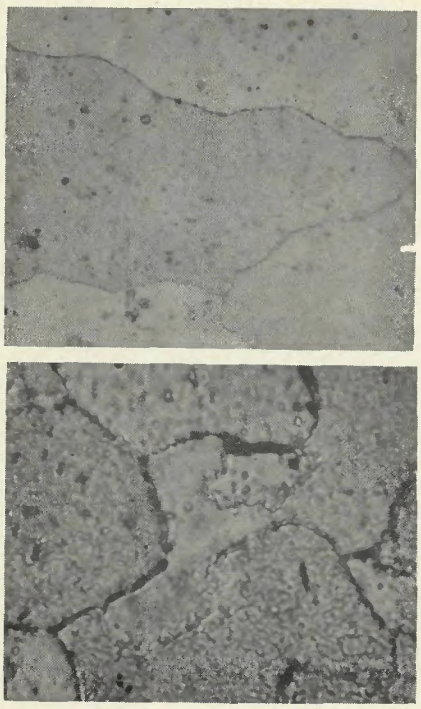

Fig. 10—7075–T6 microstructures: A (top)—specimen 4 (T = 900° F, 45 psi); B (bottom)—specimen 15 (T_p = 1050° F, 45 psi). ×2000 (reduced 41% on reproduction)

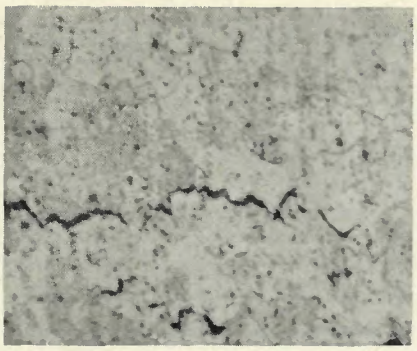

Fig. 8—Hot cracked 6061–T6 aluminum—specimen 8. ×1000 (reduced 41% on reproduction)

for 6061–T6 and 7075–T6 aluminum alloys are outlined in Table 1.[14]

The peak temperatures were selected as to fit between the equilibrium liquidus and solidus for each alloy. The peak temperatures for the 6061 alloy beagn with 1100° F and increased in 25° F increments until hot cracking occurred. The 7075 alloy peak temperatures started at 900° F and increased in 50° F increments until failure occurred. For a given peak temperature, the test specimens were cooled at four rates by varying the cooling air pressure at the manifold.

Typical cooling rates for 7075–T6 aluminum are shown in Fig. 5. The typical load-temperature recorded test data are outlined in Fig. 6. These data indicated the output generated during an experiment. Tables 2 and 3 detail the experimental data for 6061–T6 and 7075–T6 aluminum.

The cooling solidus (T_c) was determined by examining the load-time curve. When the temperature of a specimen passes through the solidus, the slope of the load curve changes more noticeably than the cooling curve. This is discussed in detail when the data are analyzed.

Microstructure

Each of the test specimens was sectioned, with a portion of the hot zone mounted and polished for metallographic examination. The polished surfaces were etched (Keller's etch) to reveal the microstructure. Fig. 7 shows low magnification (× 100) photomicrographs of the as-received 6061–T6 and 7075–T6 sheet. The 6061–T6 microstructure is typical for all 6061–T6 specimens, except for specimen 8 where obvious failure occurred. The microstructure of specimen 8 is shown in Fig. 8. The microstructure indicates definite hot cracking which is within the grain boundaries. The specimen heated to T_p and cooled indicates a thicker grain boundary than the as-received material. The more significant grain boundary is related to the liquid phase present at T_p. No significant microcracking was observed in the 6061-T6 aluminum

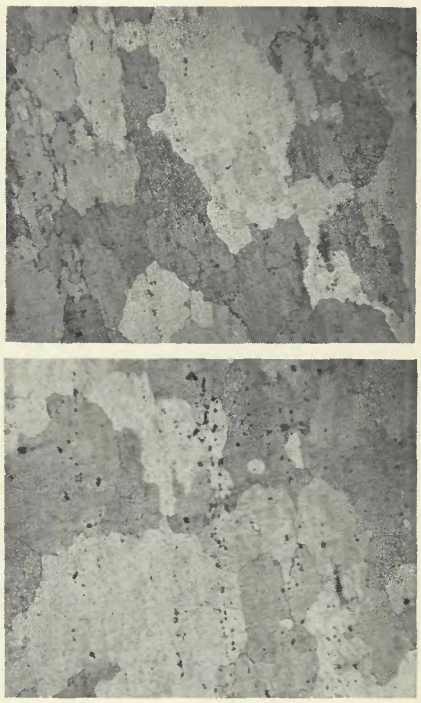

Fig. 9—7075–T6 microstructures: A (top)—specimen 4 (T_p = 900° F, 45 psi); B (bottom)—specimen 15 (T_p = 1050° F, 45 psi). ×1000 (reduced 41% on reproduction)

specimens prior to fracture.

Figure 9 shows the microstructures of a series of 7075–T6 specimens under low magnification. However, observation at high magnification indicates differences. The differences are shown in Fig. 10. The as-received specimen indicates narrow grain boundaries while specimen 15 clearly outlines the effect of the liquid phase at T_p on the grain boundary. The width of the grain boundary becomes more predominate with the greater liquid content at T_p. The extent of microcracking is related to the peak temperature and the cooling rate. Fig. 11 illustrates the intergranular nature of hot cracking failure in the heat-affected zone.

Differences between the micro-structures of 6061–T6 and 7075–T6 aluminum following test are generalized as follows:

1. The 6061–T6 grains are much smaller than the 7075–T6 grains.

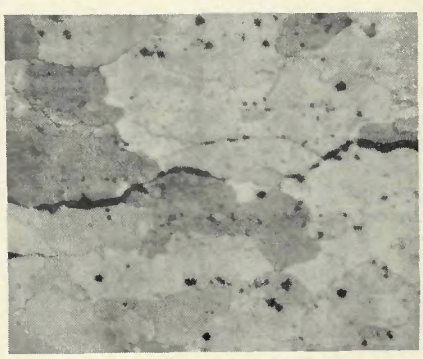

Fig. 11—Hot cracked 7075–T6 aluminum—specimen 17. ×1000 (reduced 41% on reproduction)

Table 4—Strain Data for 6061–T6 Aluminum

Specimen number	Liquid phase at T_p, %	ϵj, micro-in./in.	ϵ_c, micro-in./in.	ϵ_p, micro-in./in.
1	7.80	1716.0	1453.4	— 262.6
2	8.45	1859.0	1649.8	— 209.2
3	10.96	2411.0	2352.0	— 59.0
4	12.31	2708.0	1846.2	— 861.8
5	20.00	4400.0	1178.4	—3221.6
6	15.22	3480.0	1296.3	—2183.7
7	19.75	4344.0	1649.8	—2694.2
8	—	—	—	—
9	—	—	—	—

Table 5—Strain Data for 7075–T6 Aluminum

Specimen number	Liquid phase at T_p, %	ϵj, micro-in./in.	ϵ_c, micro-in./in.	ϵ_p, micro-in./in.
1	1.00	220.0	3535.4	3315.4
2	1.74	499.0	1402.9	903.9
3	2.12	466.0	1210.5	744.5
4	2.15	473.0	1316.7	843.7
5	1.06	223.0	3338.9	3115.9
6	3.01	663.0	1501.9	838.9
7	2.73	600.7	1404.5	803.8
8	2.81	617.7	870.7	253.0
9	2.55	561.7	3142.6	2580.9
10	3.16	696.0	1665.2	969.2
11	4.16	915.3	1596.9	681.6
12	4.26	936.0	1360.3	424.3
13	4.99	1097.7	3920.0	2732.3
14	5.45	1199.0	1366.3	167.3
15	6.25	1375.0	1350.8	— 24.2
16	6.07	1335.0	1505.8	170.8
17	—	—	—	—
18	—	—	—	—

2. The amount of grain boundary phase in the 6061–T6 specimens is much greater than that of the 7075–T6 specimens.

Discussion of Results

The data generated in the research provide significant meaning when the simulated weld results are correlated with the resultant microstructures. The assumption was to correlate the plastic strain theory with experimental data. Based on this theory, the data are reduced and recorded in Tables 4 and 5. The critical strains are thus evaluated for the proposed weld parameters above the cooling solidus temperature.

Examination of the 6061–T6 test data reveal a typical load-time plot which is shown in Fig. 12. The alloy is a relatively soft alloy and therefore would tend to be ductile and would plastically deform easily, particularly at high temperature. The portion of the curve from A to B (Fig. 12) indicates that at elevated temperatures build up of the elastic strain in the specimen is dissipated through plastic deformation. The portion of the curve from B to C indicated that the integrity of the microstructure is increasing and thus limits further plastic deformation. At point C, the load has built sufficiently that plastic deformation occurs once again. This is related to the elastic limit at elevated temperatures. The strain in this region is caused by thermal contraction and related to the $\alpha\Delta T$ function.

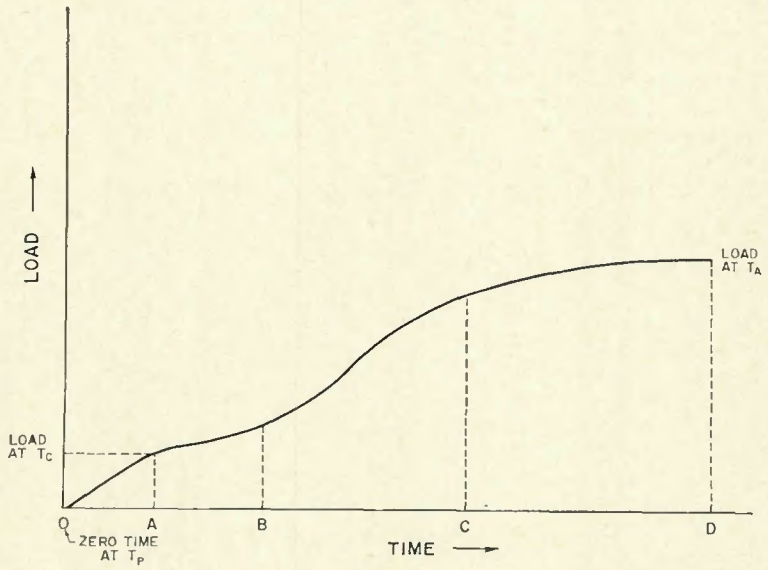

Fig. 12—Typical load curve for 6061–T6 aluminum

The microstructures of the 6061–T6 aluminum specimens show a large amount of liquid phase present in the grain boundaries. This would indicate that the 6061–T6 qlloy could deform readily above the T_c. Consequently, strain generated due to thermal contraction would be dissipated and would not lead to microcracking. This fact is substantiated by the fact that no microcracking was observed in the 6061–T6 microstructures. Fracture or hot cracking was observed only when deformation was extensive. The negative plastic strain (ϵ_p) of the alloy indicates that the heat-affected zone reacts as a viscoelastic material above the cooling solidus.

Point A in Fig. 12 was chosen as the cooling solidus temperature T_c on the basis of the strain theory. The load generated between points O and A picks up steadily indicating some restriction of plastic deformation. This would correspond directly to the interlocking action of the dendrites which permits the generation of load. When T_c is reached, the structure breaks down and plastic deformation is allowed. Further thermal contraction of the specimen restricts plastic flow and integrity is restored to the structure.

The experimental data generated for the 7075–T6 aluminum alloy, a harder alloy than 6061–T6, reveals quite different hot cracking characteristics. The load-time curves for good and microcracked specimens are shown in Fig. 13. The no microcracking curve shows load building up from 0 to A. The mechanism is basically the same as that for 6061–T6 aluminum. Once the cooling solidus has been reached, the load increase changes slope and the stress related function, $\alpha\Delta T$, becomes the controlling mechanism. The steady increase of the load-time curve would suggest that very little plastic deformation is evident. This is further substantiated by the microstructures which show large grain size and a very low percentage of liquid phase at T_p. The opportunity for plastic deformation does nor present itself above or below

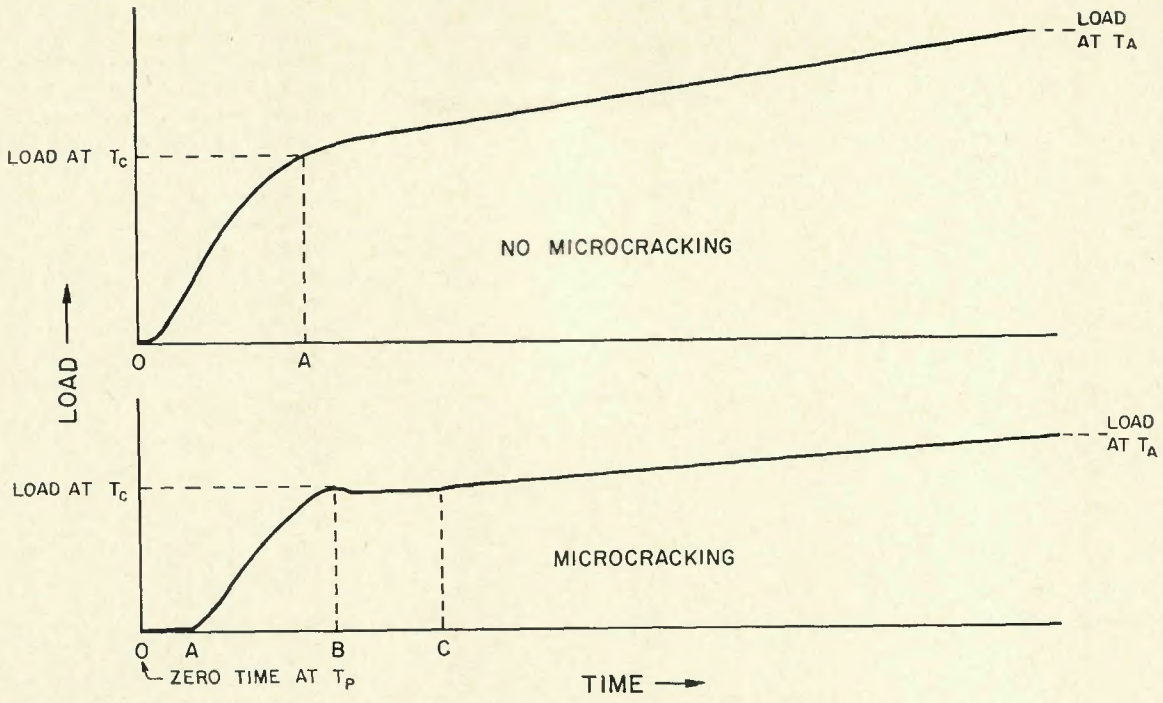

Fig. 13 —Typical load curves for 7075–T6 aluminum

the cooling solidus. The aluminum alloys now could be classified as demonstrating brittle characteristics. The brittle materials exhibit limited ductility and this is verified by the positive values of ϵ_p.

For higher temperatures and cooling rates, the characteristic load-time curves for 7075–T6 aluminum are obviously different. The portion of the curve from 0 to A is the region where there is no dendrite interlocking and thus no generated load. From point A to point B, the dendrites begin to form and interlock. At point B, the structure has completely solidified but the rapid solidification of the liquid phase has not allowed for proper deformation and microcracks are formed in the grain boundaries. Region B to C on the curve indicates microcrack propagation. The propagation is a function of the thermal strain $\alpha\Delta T$. The higher the peak temperature and the cooling rate, the longer the length of the microcrack. During the microcrack propagation, deformation of the structure is evident and produces the flat portion of the curve. The length of the plat portion of the load-time curve can be related to the extent of microcracking.

Plotting the plastic strain ϵ_p as a function of T_p and cooling rate reveals some very interesting characteristics. The 6061–T6 aluminum data are plotted in Fig. 14. Fracture occurs when the plastic deformation becomes excessive. This would suggest a viscoelastic type material which can undergo very large deformation with little generation of

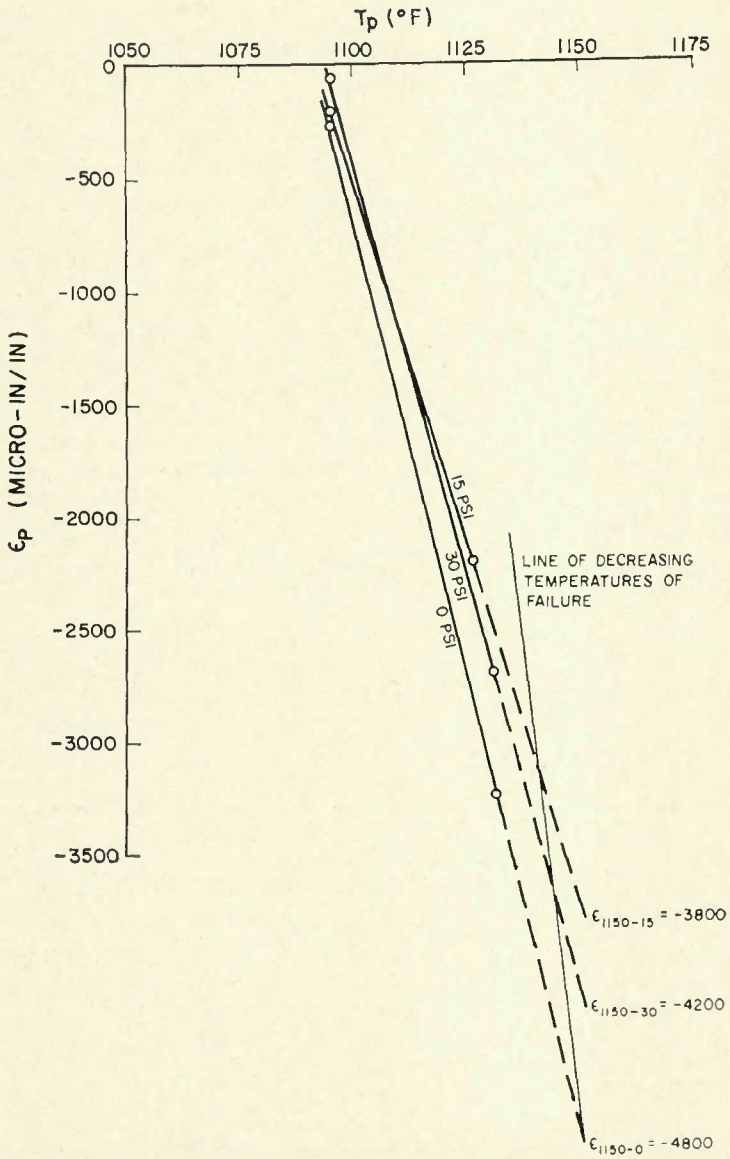

Fig. 14—T_p vs. ϵ_p for 6061–T6 aluminum

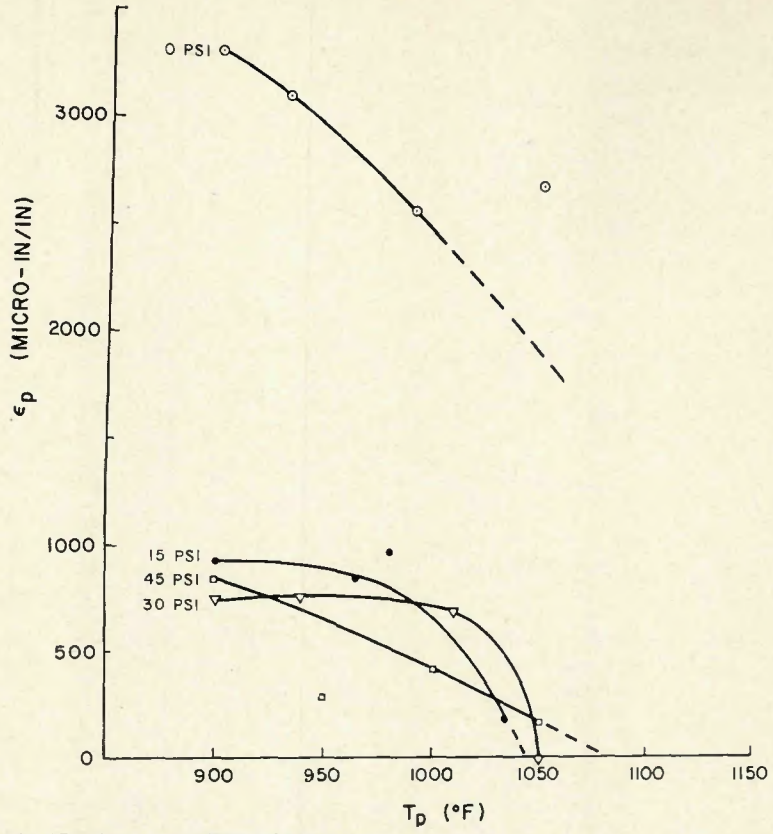

Fig. 15—T_p vs. ϵ_p for 7075-T6 aluminum

load. The material deforms until it virtually falls apart. In order for this to happen the ϵ_p would have to increase at a much greater rate than ϵ_c. This is stress-time related and would indicate critical cooling rates and peak temperatures. Increasing both of these factors lengthens the region for plastic deformation to occur. A T_p of 1132° F and a cooling of 30 psi produced ϵ_p of −2594.2 micro in./in. which is near the point of fracture for this alloy.

The behavior of the 7075-T6 aluminum specimens is shown in Fig. 15. These curves are quite different from those of the 6061-T6 specimens. The slopes of the T_p vs. ϵ_p curves decrease to a point of zero plastic strain. This indicates that as T_p increases the brittle nature of the specimen increases. Increasing cooling rates also decreases the plastic strain thus producing a more brittle material. The combination of T_p and ϵ_p provide a mechanism similar to thermal shock in ceramic materials. The brittle nature of the specimens produces microcracking along the grain boundaries and finally fracture when the plastic strain is reduced to zero.

The 6061-T6 and 7075-T6 aluminum alloys are susceptible to hot cracking through different modes. The mechanism for the generation of hot cracking during welding is plastic strain ϵ_p oriented for both alloys.

Conclusion

The information generated from this research can be summarized into several basic concepts. The thermal condition of the weld heat-affected zone produces a strain state which can be directly correlated with the condition of the microstructure. Secondly, the plastic strain ϵ_p is the governing strain for hot cracking. Plastic strains may be obtained which represent the fracture criterion. These plastic strains determine the mode of failure for a given aluminum alloy in the hot cracking region. Crack susceptibility would be greater with a brittle material than with a viscoelastic material

This research has provided the basic ground work for a technical understanding of hot cracking of welded materials. The critical plastic strains for fracture should be established for other aluminum alloys and other classes of metals which demonstrate the hot cracking phenomenon. From these studies, a mathematical relationship between plastic and elastic strains above T_c can be firmly formulated.

References

1. Kammer, P. A., Masubuchi, K., and Monroe, R. E., "Cracking in High-Strength Steel Weldments—A Critical Review," DMIC 197, Battelle Memorial Institute, February 1964.
2. Savage, W. F., and Krantz, B. M., "An Investigation of Hot Cracking in Hastelloy X," WELDING JOURNAL, 45 (1), Research Suppl., 13-s to 25-s (1966).
3. Borland, J. C., and Younger, R. N., "Some Aspects of Cracking in Cr-Ni Austenite Steels," *British Welding Journal*, (1960).
4. Williams, A. J., Rieppel, P. J., and Voldrich, C. B., "Literature Survey on Weld-Metal Cracking," WADC-TR 52-143 Wright-Paterson Air Force Base, Ohio.
5. Duvall, D. S., and Owczarski, W. A., "Further Heat-Affected-Zone Studies in Heat-Resistant Nickel Alloys," WELDING JOURNAL, 46 (9), Research Suppl., 423-s to 432-s (1967).
6. *Welding Handbook*, Fourth Edition, Section 1, A.W.S., New York, N. Y., 1957.
7. Savage, W. F., and Lundin, C. D., "The Varestraint Test," WELDING JOURNAL, 44 (10), Research Suppl., 433-s to 442-s (1965).
8. Movehan, B. A., "Mechanism and Causes of Hot Cracking in Welds," *Avtom. Svarka*, 12 (6), 59-81 (1959).
9. Pumphrey, W. I., and Jennings, P. H., "A Consideration of the Nature of Brittleness at Temperatures Above the Solidus in Castings and Welds in Aluminum Alloys," *Journal of the Institute of Metals*, 75 235-236 (1948).
10. Pellini, W. S., "Strain Theory of Hot Tearing," *Foundry*, 80 (11), 124-132 (1952).
11. Borland, J. C., "Generalized Theory of Super-Solidus Cracking in Welds (and Castings)," *British Welding Journal*, 7 (8), 508-512 (1960).
12. Bell, J. R., "A Study of the Relationship of Microsegregation to Cracking in Constructional Alloy Steels," Thesis to Department of Materials Engineering, Rensselaer Polytechnic Institute, March 1966.
13. Wells, R. L., "A Study of Cracking During Welding of Aluminum Alloys," *Journal of Basic Engineering*, Transactions of the ASME, 89 (1), 40-48 (1967).
14. *Welding Handbook*, Eighth Edition, Vol. 1, A.W.S., 1961.